ARGONNE NATIONAL LABORATORY
9700 South Cass Avenue, Argonne, Illinois 60439

A Theoretical Model for the Irradiation-Enhanced Interdiffusion of Al and U Alloys*

J. Rest
Argonne National Laboratory
U.S.A

To be presented at the 23rd International Meeting on Reduced Enrichment for Research and Test Reactors, Las Vegas, Nevada, October 1-6, 2000

*Work supported by U.S. Department of Energy, Office of Arms Control and Nonproliferation, under Contract W-31-109-Eng-38.

A Theoretical Model for the Irradiation-Enhanced Interdiffusion of Al and U Alloys

J. Rest, Argonne National Laboratory, 9700 S. Cass Ave., Argonne, IL 60439, USA

Abstract

A model for the interdiffusion of Al and U alloys has been developed based on the premise that the generation of a high dislocation density leading to the formation of a cellular dislocation network provides a sufficient sink density in the material such that the sinks dominate defect behavior. The theoretical model thus derived has the following characteristics: 1. The effective interdiffusion coefficient is proportional to fission rate to the ¾ power and exponentially dependent on temperature, 2. The interstitial migration enthalpy is given by $\varepsilon_i - \varepsilon_v / 2 = 0.74eV$, and 3. The model is consistent with uranium-silicide interdiffusion data if the vacancy migration enthalpy is $\approx 0.5eV$. Finally, it is shown that the lack of SEM-resolvable bubbles in uranium aluminide is consistent with item 2, above, i.e., $\varepsilon_i - \varepsilon_v / 2 > 0$.

1. Introduction

Data on the interdiffusion of Al and uranium silicide during irradiation has resulted in an empirical correlation that expresses the thickness of the interaction zone as linearly dependent on the fission rate with an exponential temperature dependence [1]. Recent data for the interdiffusion of Al and U-10Mo is consistent with this correlation. However, these dependencies have no physical basis. In general, at the low temperatures of interest for RERTR, radiation-enhanced diffusion is dominant over thermal diffusion. In turn, the specific mechanism of radiation-enhanced diffusion (e.g. of Al in UAl_x) is dependent on the defect properties in the material. If the defect lifetimes are dominated by pair annihilation then radiation-enhanced diffusion is proportional to the square root of the fission rate with exponential temperature dependence. On the other hand, if the defect lifetimes are dominated by their interaction with sinks (e.g., a fixed density of dislocations), then the predicted dependence is linear with fission rate and athermal.

The dependence of the interdiffusion distance on fission rate and temperature are similar for U_3Si, U_3Si_2, and, based on data available thus far, U-10Mo. A possible basis for these similarities is the hypothesis that diffusion of Al through the aluminide is the dominant mechanism in the formation of the aluminide reaction layer.

A model for the interdiffusion of Al and U alloys has been developed based on the premise that the generation of a high dislocation density leading to the formation of a cellular dislocation network provides a sufficient sink density in the material such that the sinks dominate defect behavior. Most models for irradiation-enhanced diffusion appearing in the open literature treat the sink density as constant and independent of temperature. However, in general, the steady-state dislocation density is dependent on temperature.

The theoretical model thus derived has the following characteristics:

1. The effective interdiffusion coefficient is proportional to fission rate to the ¾ power and exponentially dependent on temperature.
2. The interstitial migration enthalpy is given by $\varepsilon_i - \varepsilon_v / 2 = 0.74eV$.
3. The model is consistent with uranium-silicide interdiffusion data if the vacancy migration enthalpy is $\approx 0.5eV$.

Another interesting aspect of uranium aluminides is that no SEM-resolvable bubbles have been observed in irradiated UAl_x materials [2]. Based on experience with oxides, silicides, and now, uranium alloys, the lack of observable bubbles in the aluminides can be postulated to be due to the absence of recrystallization. Theoretical calculations for irradiation-induced recrystallization, using models that are currently under development, indicate that the absence of recrystallization in aluminides can be understood if the interstitial migration enthalpy is greater than one half the vacancy migration enthalpy, that is the very same condition that is imposed for the interdiffusion calculation.

2. Model

The equilibrium concentration of mobile point defects within the bulk material, C_v and C_i, can be determined from the rate equations that describe point–defect behavior, which, for negligible bulk diffusion (e.g., to a surface) are given by

$$\frac{\partial c_v}{\partial t} = K - K_{iv} c_i c_v - K_{sv} s_v c_v , \quad (1)$$

and

$$\frac{\partial c_i}{\partial t} = K - K_{iv} c_i c_v - K_{si} s_i c_i , \quad (2)$$

where K is the damage rate in dpa/s ($K = \dot{f} / C_{fK}$, where $\dot{f}$ is the fission rate and $C_{fK} \approx 5x10^{17}$ fissions/dpa) and K_{iv}, K_{sv}, and K_{si} are the rate coefficients for mutual recombination and for the annihilation of vacancies and interstitials at sinks. Here the assumption is made that the overall effect of solute concentration on the steady-state concentration of point defects is small. The sinks, which occupy time-independent fractions of the lattice nuclei, are assumed to be inexhaustible and randomly distributed. The rate coefficients are

$$K_{iv} = 4\pi r_{iv} (D_i + D_v) / \Omega \cong 4\pi r_{iv} D_i / \Omega , \quad (3)$$

$$K_{sv} = 4\pi r_{sv} D_v / \Omega , \quad (4)$$

$$K_{si} = 4\pi r_{si} D_i / \Omega . \quad (5)$$

Here, r_{iv} is the radius of the recombination volume; r_{sv} and r_{si} are annihilation radii and depend on the type of sink, e.g., dislocation line, jog, or microvoid; and D_v and D_i are the random-walk diffusion coefficients of vacancies and interstitials given by

$$D_v = a^2 \omega_0^v , \quad (6)$$

$$D_i = \frac{2}{3} a^2 \omega_0^i , \quad (7)$$

where

$$\omega_0^v = \upsilon_v \, e^{-\varepsilon_v / kT} , \quad (8)$$

and

$$\omega_0^i = \upsilon_i \; e^{-\varepsilon_i / kT}, \tag{9}$$

where ε_v, ε_i and υ_v, υ_i are the migration energies and vibration–frequency factors for vacancies and interstitials, respectively.

Before proceeding, we must establish criteria to determine when mutual recombination of point defects dominates annihilation at internal sinks, and when the loss of vacancy-impurity pairs by recombination with interstitials dominates pair loss due to dissociation (i.e., vacancy emission). If the assumption is made that $s_v \approx s_i$, the solution to Eqs. 1 and 2 is given by

$$D_v c_v = D_i c_i = (K/f_0^{1/2})\left[(1+Q)^{1/2} - Q^{1/2}\right], \tag{10}$$

where $2D_v c_v$ is the radiation-enhanced diffusion coefficient, and

$$Q = \frac{s_i^{\,2} K_{s\,i}^{\,2} D_v}{4K K_{i\,v} D_i}, \tag{11}$$

and

$$f_0 = \frac{K K_{i\,v}}{D_i D_v}. \tag{12}$$

For values of K and s_i such that $Q << 1$ mutual recombination of defects is dominant over annihilation at internal sinks (i.e., the 2nd term on the right-hand-side of Eqs. 1 and 2 is much larger than the 3rd term), and leads to

$$D_v c_v = D_i c_i = \left(\frac{K D_i D_v}{K_{i\,v}}\right)^{1/2}. \tag{13}$$

From Eq. 13 it is seen that $Q << 1$ leads to a radiation-enhanced diffusion coefficient that has exponential temperature dependence and is proportional to the square root of the fission rate. On the other hand, for values of K and s_i such that $Q >> 1$ annihilation of defects at internal sinks is dominant over mutual

recombination (i.e., the 2nd term on the right-hand-side of Eqs. 1 and 2 is much smaller than the 3rd term), leading to

$$D_v c_v = D_i c_i = \frac{KD_i}{s_i K_{s\,i}} = \frac{KD_v}{s_v K_{s\,v}} . \tag{14}$$

From Eq. 14 it is seen that the combination of $Q >> 1$ and constant s_i leads to a radiation-enhanced diffusion coefficient that is temperature independent and linearly dependent on fission rate. However, in most cases the assumption (used widely in the literature) of constant sink density s_i is incorrect.

A rate-theory-based model has been used to investigate the nucleation and growth of cavities during low-temperature irradiation of UO_2 in the presence of irradiation-induced interstitial-loop formation and growth [3]. Consolidation of the dislocation structure takes into account the generation of forest dislocations and capture of interstitial dislocation loops. The loops accumulate and ultimately evolve into a low-energy cellular dislocation structure. Interstitial loop growth continues until a cellular dislocation microstructure forms, i.e.,

$$g(t) = C_A C_\rho \sqrt{\frac{\pi}{f(\upsilon)}} - d_l(t)\sqrt{\rho_l(t)} = 0 , \tag{15}$$

where $f(\upsilon) = \frac{1-\upsilon/2}{1-\upsilon}$, υ is Poisson's ratio (0.31), $C_A = 3$ for cubic cells and C_ρ is within a factor of 2 or so either way of unity. The condition given by Eq. 15 is obtained by minimization of the total energy (dislocation line energy plus the energy stored in isolated terminating dislocation boundaries). Once Eq. 15 is satisfied it is assumed that a stable cellular dislocation microstructure with a fixed cell size has been attained. In reality, the continued pileup of dislocations on the cell walls will result in a decrease in cell size in order to maintain the lowest energy configuration.

The condition for the formation of a cellular dislocation microstructure, Eq. 15, results in an expression for the cell size as a function of the dislocation density, i.e.,

$$\mathrm{d}_l(t) = \frac{\mathrm{C_A C}_\rho}{f(\upsilon)} \sqrt{\frac{\pi}{\rho_m(t)}}. \tag{16}$$

The steady-state mobile dislocation density can be expressed as [4]

$$\rho_m(t) = \left(\frac{3}{La}\right)^{2/3} \left(\frac{KD_\mathrm{v}}{\alpha_r}\right)^{1/6} \left(\frac{\alpha_i}{BD_i}\right)^{1/3}, \tag{17}$$

where $\alpha_i = \sqrt{2}/a^2$ is the rate constant for nucleation of loops as di-interstitials, $\alpha_r = 4\pi r_{\mathrm{iv}}/\Omega$ is the rate constant for loss of defects due to recombination, a is the lattice constant, Ω is the atomic volume, L is the cell size, and B is the relative bias given by $Z_i - Z_\mathrm{v} = 4\pi\left(r_{si} - r_{sv}\right)/\left(\Omega\rho_A\right)$ with ρ_A the atom density of the material.

Combining Eqs. 16 and 17 results in

$$\mathrm{d}_l(t) = \frac{\mathrm{C_A C}_\rho}{f(\upsilon)} \sqrt{\frac{\pi}{\left(\frac{3}{La}\right)^{2/3} \left(\frac{KD_\mathrm{v}}{\alpha_r}\right)^{1/6} \left(\frac{\alpha_i}{BD_i}\right)^{1/3}}}. \tag{18}$$

If we identify the sink density in this system as the density of cell corners, or so-called triple points, then the sink density $\mathrm{c_s}$, is given by $1/\mathrm{d}_l^3$, i.e.,

$$c_s = \frac{\left(\frac{3}{La}\right)^2 \left(\frac{1}{\alpha_r}\right)^{1/2} \frac{\alpha_i}{B_i} K^{1/4} D_\mathrm{v}^{1/4} f(\upsilon)^3}{\left(\mathrm{C_A C}_\rho \sqrt{\pi}\right)^3 D_\mathrm{i}^{1/2}}. \tag{19}$$

It is important to note that the derivation of Eq. 17 for the steady-state mobile dislocation density is dependent on the assumption of $Q << 1$ (recombination is dominant). Prior to the formation of a cellular dislocation network, the sink density in the material has not reached values that would facilitate sink-dominated kinetics over recombination. However, once the microstructure reaches dislocation densities commensurate with a cellular dislocation network, defect kinetics transition from recombination to sink dominated. If we now assume that irradiation-enhanced diffusion of Al through the reaction layer is a rate controlling step in the formation of new reaction product, and that defect behavior in the reaction product is dominated by loss to sinks, then the Al interdiffusion coefficient is given by combining Eqs. 5, 14 and 19, i.e.,

$$D_{Al}=2D_v c_v = \frac{\sqrt{\pi}\left(\dot{f}/C_{fK}\right)^{3/4}\rho_A B_i L^2 a^2 \Omega\left(C_A C_\rho\right)^3 \alpha_r^{1/2} D_i^{1/2}}{18 r_{s\,i} f(\upsilon)^3 \alpha_i D_v^{1/4}}, \qquad (20)$$

where in Eq. 14, $s_v = c_s / \rho_A$.

Eq. 20 is a major result of this analysis. The Al irradiation-enhanced effective interdiffusion coefficient given by Eq. 20 is dependent on the fission rate to the ¾ power, and is exponentially dependent on temperature with the activation enthalpy given by $(\varepsilon_i - \varepsilon_v/2)/2$.

3. Results

Fig. 1 shows the results of regression analysis of reaction layer thickness data for U_3Si_2-Al as a function of irradiation temperature. Regression analysis was implemented assuming that the effective interdiffusion coefficient is proportional to fission rate to the ¾ power and exponentially dependent on temperature. The activation enthalpy for diffusion is 8520 calories. Fig. 2 shows the results of applying the fit determined in Fig. 1 to U_3Si_2-Al and U_3Si-Al interaction layer data. Also shown in Fig. 2 is the variation in predicted results using the fit for a $\pm$ 25K variation in irradiation temperature. The results shown in Fig. 2 demonstrate that the fission rate dependence predicted by sink-dominated kinetics derived in Section 2 is consistent with observations on these silicide fuels.

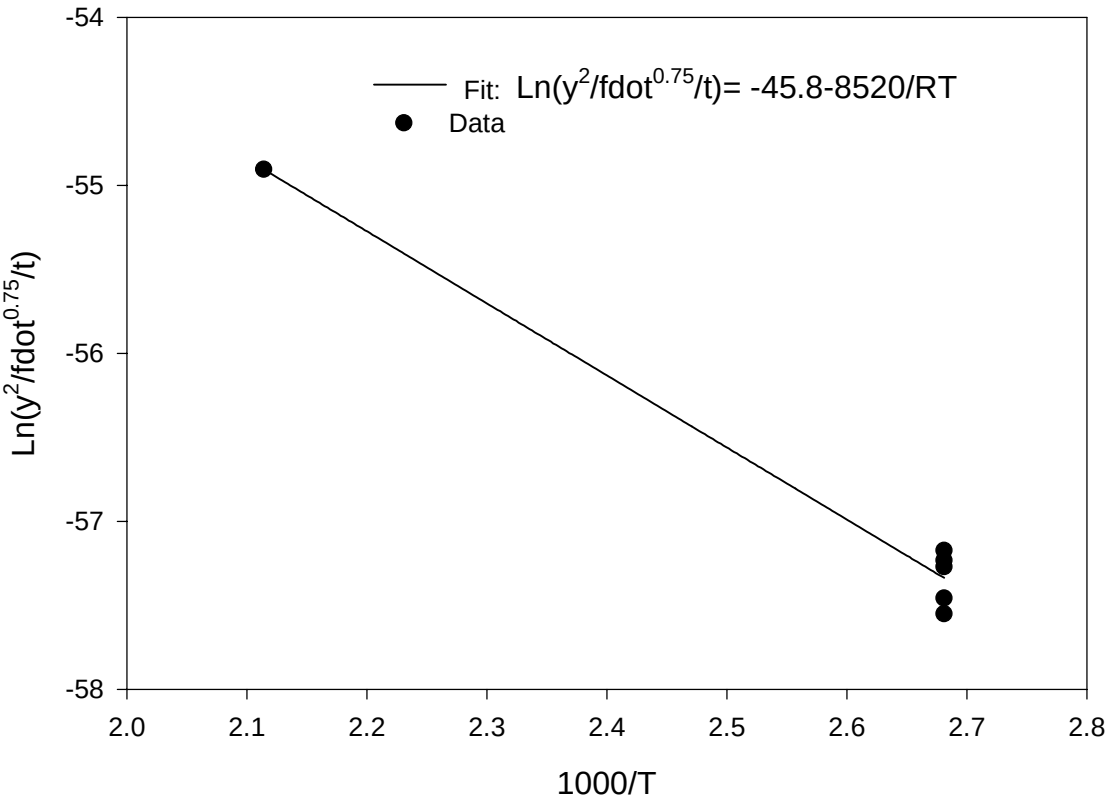

Fig. 1 Regression analysis of reaction layer thickness data, y, for U_3Si_2-Al as a function of irradiation temperature. fdot is the fission rate and t is the irradiation time.

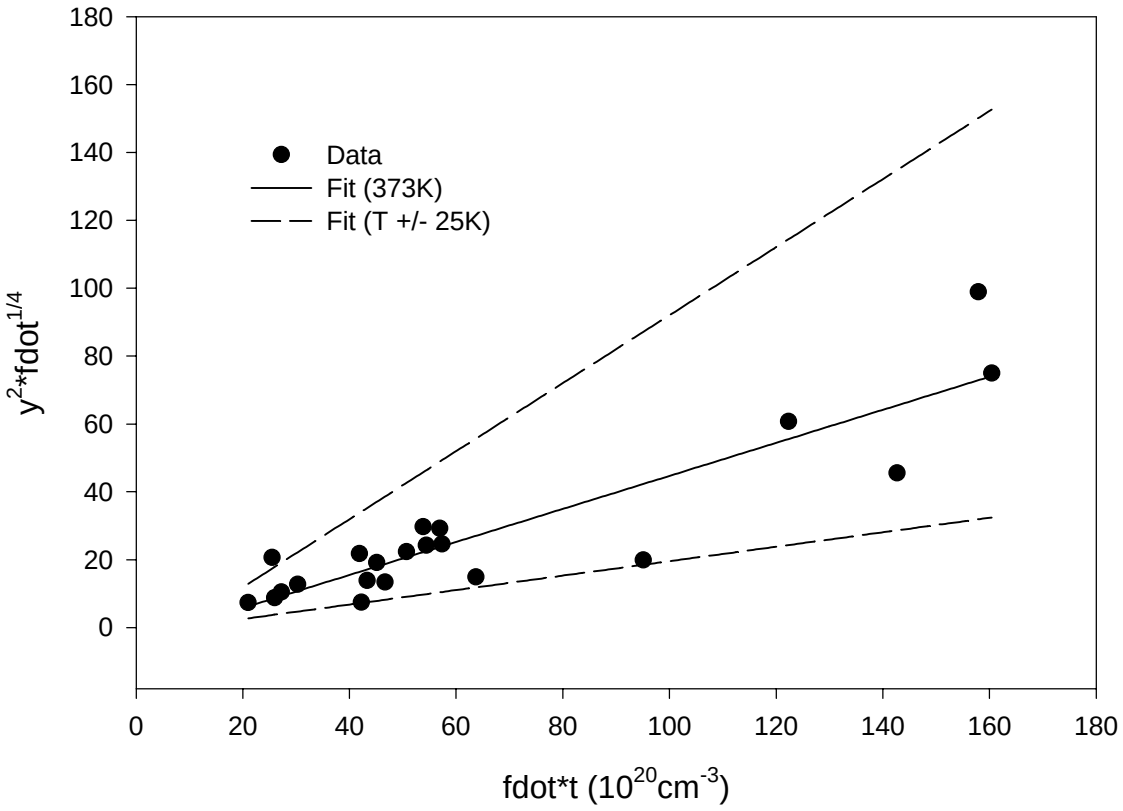

Fig. 2 Results of applying the fit determined in Fig. 1 to U_3Si_2-Al and U_3Si-Al interaction layer thickness data as a function of irradiation dose. Also shown in Fig. 2 is the variation in predicted results using the fit for a $\pm$ 25K variation in irradiation temperature.

Identifying the effective interdiffusion activation enthalpy determined in Fig. 1 with $(\varepsilon_i - \varepsilon_v / 2)/2$ from Eq. 20,

$$\varepsilon_i - \varepsilon_v / 2 = 0.74eV \,. \tag{21}$$

For example, if $\varepsilon_v = 0.5eV$, then Eq. 21 gives $\varepsilon_i = 0.99eV$. This set of values for the defect migration enthalpies is unusual in that in many materials, such as pure metals, the interstitial is the fastest moving

species at low temperature. However, there are materials where the situation is reversed, e.g., in ordered materials such as concentrated $\alpha - AgZn$ alloys. In Ag-30-at.%Zn the vacancy and interstitial enthalpies were measured to be $0.56 \pm 0.02eV$ and $0.94 \pm 0.02eV$, respectively [5]. It is important to check that the values for the defect migration enthalpies are consistent with the assumption of sink-dominated defect behavior, i.e., the use of Eq. 14. In order to perform this check, various parameters appearing in Eq. 20 have to be assigned values. The values of these parameters are listed in Table 1.

Table 1. Values of various parameters used in Eq. 20

Parameter	Value
r_{iv}	3×10^{-8} cm
ε_v	0.5eV
C_ρ	2
B	0.03
a	5.0×10^{-8} cm
r_{sv}	2×10^{-8} cm
ρ_A	a^{-3}
ν_v	5×10^{13} s^{-1}
υ_i	5×10^{14} s^{-1}
Ω	a^3
L	3×10^{-5} cm

Using the values of parameters listed in Table 1, for a fission rate of 8×10^{15} $cm^{-3}s^{-1}$ and irradiation temperature of 373-423K (e.g., HFIR) $Q \approx 7-28$. For 373K and a fission rate of 2×10^{14} $cm^{-3}s^{-1}$ (e.g., ORR) $Q \approx 44$. Thus, the values for the defect migration enthalpies used in the model are consistent with the assumption of sink-dominated defect behavior . The value of L listed in Table 1 is somewhat larger

than the cell size calculated using Eq. 16, i.e., $d_l \approx 10^{-6} cm$. In Table 1, the effective lattice parameter has been chosen to reflect the assumption that Al diffuses on the Al-Si sub lattice of the $U_3Al_7Si_2$ interaction-layer compound.

Defining the depth of the interaction layer as

$$Y_{\text{int}} = \sqrt{D_{Al} t}\,, \tag{22}$$

Eqs. 21 and 22 with the values listed in Table 1 are consistent with the solid line fit shown in Fig. 2.

4. Relationship of Sink-Dominated Diffusion Kinetics to lack of Observable bubbles in UAl_x

In general, bubbles resolvable with a SEM have not been observed in UAl_x [2]. Bubbles confined to the bulk (lattice) material cannot grow to appreciable sizes at low temperatures due to the effect of irradiation-induced re-solution. Only when sinks, such as grain boundaries, are present in the material can bubbles grow to observable sizes. The strong sink-like nature of a grain boundary provides a relatively short recapture distance for gas that has been knocked out of a bubble due to re-solution, and as such neutralizes the "shrinking" effect of the re-solution process. These grain-boundary bubbles grow at an enhanced rate as compared to those in the bulk material.

Irradiation-induced recrystallization provides new grain boundaries upon which bubbles can nucleate and grow at an accelerated rate. Prior to recrystallization, bubbles are generally not observed in uranium alloy fuels. If recrystallization does not occur in UAl_x, then this would offer a basis for understanding the absence of such bubbles in SEM micrographs of the irradiated material.

Equation 19 gives the density of cell corners, or so-called triple points in the irradiated UAl_x. In previous work [6], cellular dislocation walls were postulated to be potential nuclei for recrystallization. The stored energy in the material is concentrated on the cell walls. The fraction of immobile walls increases with dose due to interaction with mobile, irradiation-produced impurities (i.e., vacancy-solute

pairs). A possible candidate for such an impurity is a fission-gas atom. The equilibrium number of nuclei per unit volume is given by

$$c_s^* = c_s^0 \exp[-\Delta G^* / kT], \tag{23}$$

where ΔG^* is the critical standard free energy that a nucleus must acquire in order to remain a viable nucleus for recrystallization. Comparing Eqs. 19 and 23, let us identify

$$\Delta G^* = \frac{1}{2}\left(\varepsilon_v / 2 - \varepsilon_i\right). \tag{24}$$

Thus, if $\varepsilon_i > \varepsilon_v / 2$, ΔG^* is negative and recrystallization cannot occur. But this is the very same condition expressed by Eq. 21 for the sink-dominated irradiation-enhanced interdiffusion of Al through UAl_x! Thus, in order for the observed fission rate and temperature dependence of the interdiffusion of Al through UAl_x to be consistent with sink-dominated kinetics a condition is required between two materials properties (ε_v and ε_i). This very same condition precludes irradiation-induced recrystallization from occurring in the material and presumably is the basis for the lack of SEM resolvable bubbles in UAl_x.

Observations of photomicrographs of U_3Si_2 fuel particles dispersed in an aluminum powder and irradiated in the HFIR have revealed a microstructure of an outer aluminide shell (e.g., a UAl_3-type structure) that shows no evidence of grain recrystallization (Region 1 of Fig. 3F), an inner aluminide-type annulus that shows evidence of grain recrystallization (Region 2 of Figs. 3F, and Fig 3C), and a central region that shows swelling that is characteristic of an amorphous material (Region 3 of Fig. 3F). DART analysis [1,7] of the evolution and swelling of this complex microstructure has identified the following phenomena. The formation of the outer aluminide shell acts as a restraint on the swelling of the inner fuel material. This is because the outer (unrestructured) aluminide shell contains predominantly small (not visible by SEM) intragranular bubbles (Fig. 3D). Thus, this outer shell has a relatively low swelling rate when compared with the interior regions (which are composed of recrystallized and/or amorphous-like

material) and appears “hard,” or stiff, when compared with the relatively “soft,” or ductile interior regions. DART calculations show that if the outer aluminide shell does not form (e.g., for fuel particles irradiated in the absence of aluminum), fuel particle swelling rates increase significantly. Thus, for DART to generate an aluminide outer shell, aluminum diffusion into the material (i.e., through the outer fuel ring defined in the multinode configuration of the calculations) must occur before the recrystallization model predicts grain recrystallization in that node.

The inner nodes recrystallize prior to aluminum penetration, leading to an aluminide annulus with a refined grain structure (Region 2 of Figs. 3F and C). DART-calculated swelling rates in an annulus that has a refined grain structure are significantly higher (Fig. 3A) than what would occur in the absence of recrystallization (i.e., in the aluminide region, Fig. 3D) due to enhanced bubble growth on grain boundaries and on dead-end nodes. Subsequent to recrystallization, aluminum penetration of this inner annulus occurs, converting the material to a restructured (with a refined grain structure) aluminide region (Region 2 of Figs. 3F and C).

Conclusions

The dependence of the interdiffusion distance on fission rate and temperature are similar for U_3Si, U_3Si_2, and, based on data available thus far, U-10Mo. A possible basis for these similarities is the hypothesis that diffusion of Al through the aluminide is the dominant mechanism in the formation of the aluminide reaction layer. A model for the interdiffusion of Al and U alloys has been developed based on the premise that the generation of a high dislocation density leading to the formation of a cellular dislocation network provides a sufficient sink density in the material such that the sinks dominate defect behavior. Most models for irradiation-enhanced diffusion appearing in the open literature treat the sink density as constant and independent of temperature. However, in general, the steady-state dislocation density is dependent on temperature. The theoretical model thus derived has the following characteristics:

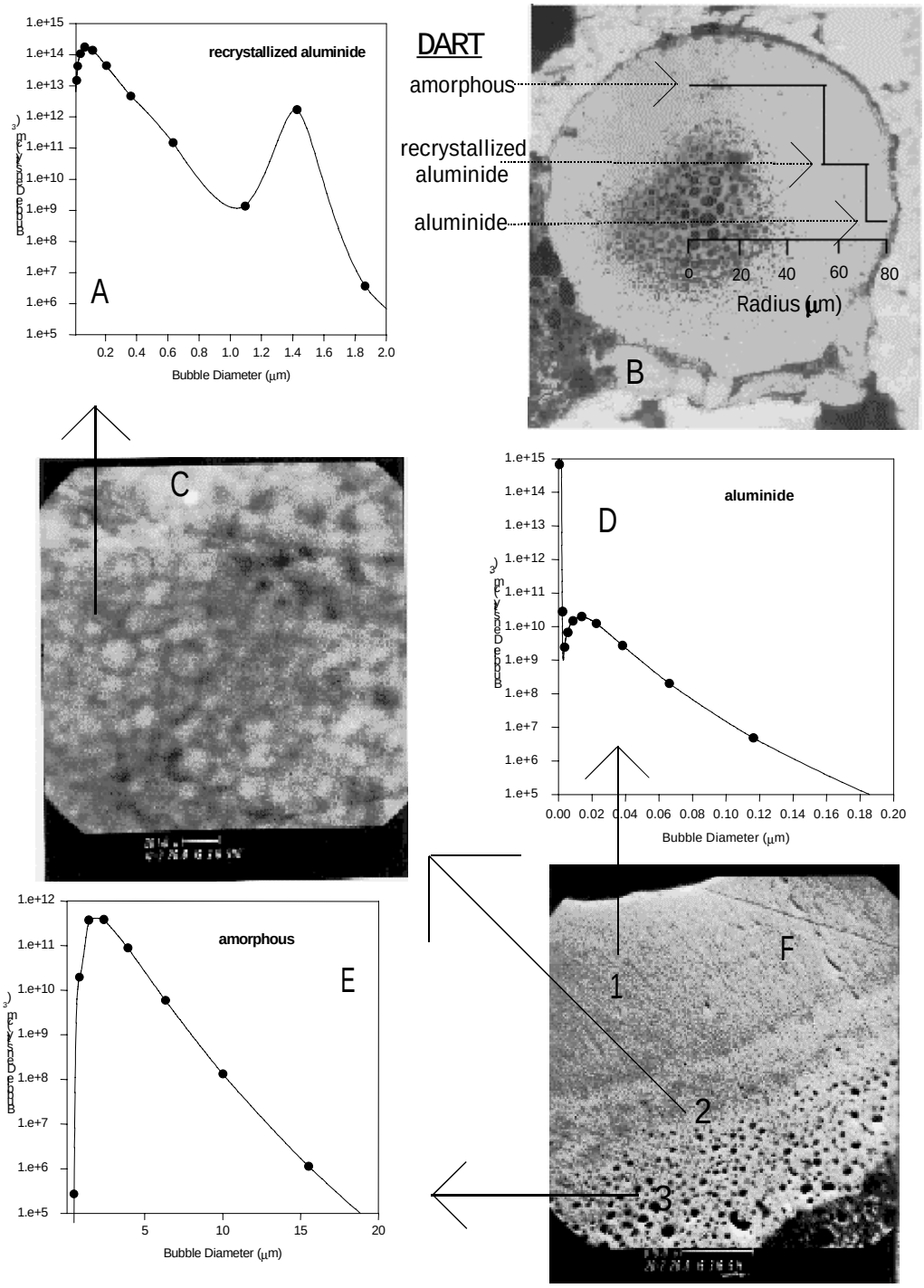

Fig. 3. DART interpretation of U_3Si_2 particle irradiation in HFIR

1. The effective interdiffusion coefficient is proportional to fission rate to the ¾ power and exponentially dependent on temperature.

2. The interstitial migration enthalpy is given by $\varepsilon_i - \varepsilon_v / 2 = 0.74eV$.

3. The model is consistent with uranium-silicide interdiffusion data if the vacancy migration enthalpy is $\approx 0.5eV$.

Another interesting aspect of uranium aluminides is that no bubbles have been observed in irradiated UAl_x materials. Based on experience with oxides, silicides, and now, uranium alloys, the lack of observable bubbles in the aluminides can be postulated to be due to the absence of recrystallization. Theoretical calculations for irradiation-induced recrystallization, using models that are currently under development, indicate that the absence of recrystallization in aluminides can be understood if the interstitial migration enthalpy is greater than one half the vacancy migration enthalpy, that is the very same condition that is imposed for the interdiffusion calculation.

References

1. J. Rest and G. L. Hofman, Nucl. Technol., **126**, 88-101 (1999).

2. G. L. Hofman, Nucl. Technol., **77**, 110 (1987).

3. J. Rest and G. L. Hofman, J. Nucl. Mater., **277**, 231-238 (2000).

4. I. Konovalov, Bochvar Institute, Moscow, Russia, Personal Communication, 1999.

5. M. Halbwachs and J. Hillairet, Phys. Rev.B **18**,4927 (1978).

6. J. Rest and G. L. Hofman, J. Nucl. Mater., **210**, 187 (1994).

7. J. Rest, "The DART Dispersion Analysis Research Tool: A Mechanistic Model for Predicting Fission-Product-Induced Swelling of Aluminum Dispersion Fuels," ANL-95/36, Argonne National Laboratory (Aug. 1995).